Automated Optic Nerve Head Image Fusion of Nonhuman Primate Eyes Using Heuristic Optimization Algorithm

Hua Cao, Bahram Khoobehi, and S. S. Iyengar, *Fellow, IEEE*

Abstract - **Multi-sensor biomedical image registration and fusion usually require intensive computational effort. This article presented a novel automated approach of the multi-sensor retinal optic nerve head image registration and fusion using heuristic optimization algorithm. The reference and the to-be-registered images are from two different modalities, i.e. angiogram grayscale images and fundus color images. The optic nerve head vasculature is extracted using Canny Edge Detector. Control points are detected at the vessel bifurcations using adaptive exploratory algorithm. Mutual-Pixel-Count (MPC) maximization based heuristic optimization adjusts the control points at the sub-pixel level. The iteration stops either when MPC reaches the maximum value, or when the maximum allowable loop count is reached. A refinement of the parameter set is obtained at the end of each loop, and finally an optimal fused image is generated at the end of the iteration. Comparative evaluation is performed with the genetic algorithm. The results show the advantages of the presented method in terms of novelty, efficiency and accuracy.**

Index Terms — Biomedical Imaging, Image Registration, Image Fusion, Mutual-Pixel-Count, Heuristic Optimization.

I. Introduction

RETINA is a nerve layer lying at the back of the eye that can sense the light passing through the lens and sends it to the optic nerve and the brain. Retinopathy, which is usually due to the damage to the blood vessels next to the retina, relates to various diseases and disorders of the retina. It is critical to treat eye diseases or injuries that affect the retina at the early stage. In practical clinical applications, the comparison of angiogram grayscale images with fundus color images is often required in order to identify dynamic aspects of the circulation and evaluate various retinal vascular disorders. Early detection can allow timely treatment to prevent further vision loss, and prolongs effective years of usable vision. The proposed approach provides a convenient way for the early detection of the retinal abnormalities, and hereby reduces the incidence of irreversible vision loss. The benefits include blindness prevention, patient care improvement, better physician, and caregiver efficiency in the eye clinic.

The most widely used methods for medical image registration and fusion are area-based and feature-based. These methods include feature extraction, segmentation, classification, pattern recognition, statistical measurements, texture analysis, and a wide variety of other approaches [2]. There is no uniform image registration algorithm that can be applied for all different cases. Mutual Information (MI) [1] is the frequently used optimization measurement in area-based fusion. This study employed the MI concept and simplified it to Mutual-Pixel-Count (MPC). MPC measures the overlap pixels of the optic nerve head vasculature. If the images are geometrically aligned, MPC represents the maximal pixel. The feature-based fusion method extracts and matches the common structures (features) from two images. The feature means the salient structures, such as the central line of vessels and the vessel bifurcation points in the retinal network. The feature-based and area-based methods are combined in this study.

II. Image Acquisition from Nonhuman Primate Eyes

The retinal optic nerve head (ONH) and overlying vessels in cynomolgus monkey eyes were imaged with a Topcon TRC-50EX fundus camera attached to a hyperspectral imaging system (Fig.1) [11]. The primates were cynomolgus monkeys of 4 to 4.5 years of age and 2.5 to 3 kg body weight with normal eyes [5]. The experimental monkey was anesthetized with the intramuscular ketamine (7-10mg/kg), xylazine(0.6-1 mg/kg), and intravenous pentobarbital (25-30 mg/kg). Administration of the anesthetics was repeated alternately every 30 minutes as required to maintain the animal in deep, stage IV anesthesia [5]. Retinal images were obtained with inspiration of pure oxygen and room air at the controlled intraocular pressures of 10 mm Hg sustained for up to 10 minutes after the eyes were dilated. Establishing animal models is an essential prerequisite of the development of new therapeutic interventions on human diseases. Monkey species provide appropriate preclinical models that can closely reflect human's physical and physiological characteristics because of their very close phylogenetic relationship with human beings.

Manuscript received April 7, 2008. This work was supported in part by the BCVC programs.

Hua Cao is with Computer Science Department, Louisiana State University, Baton Rouge, LA 70802 USA (phone: 225-324-2438; e-mail: hcao@csc.lsu.edu).

S. S. Iyengar is with Computer Science Department, Louisiana State University, Baton Rouge, LA 70802 USA (email: iyengar@csc.lsu.edu)

Bahram Khoobehi is with Department of Ophthalmology, LSU Eye Center, New Orleans, LA 70112 USA (email: BKhoob@lsuhsc.edu)

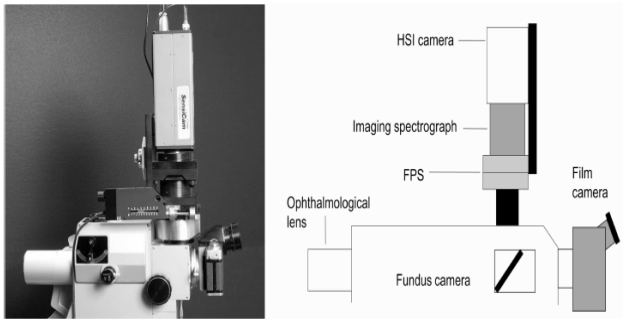

Fig. 1. Hyperspectral imaging system in relation to the fundus camera [11]

III. Vasculature Edge And Control Point Detection

A. Image Binarization

A global adaptive threshold developed by Otsu [7][8] is employed to convert the gray level colors to black-and-white. The threshold is a normalized intensity value that lies in the range [0, 1]. Otsu's method chooses the optimal threshold to minimize the intraclass variance of the black and white pixels and to maximize between-class variance in a grayscale image. The algorithm caculates the statistics of the image itself to set the threshold and use the histogram to choose its value at some percentile as a reference value of region strength. Therefore, Otsu's method is non-parametric and non-supervised.

B. Vasculature Extraction Using Canny Edge Detector

Canny Edge Detector [9] is employed to extract the optic nerve head vasculature from the binary images (Fig.2). Canny's method detects the edges at the zero-crossings of the second directional derivative of the image. In order to make the localization of magnitude maxima accurate, a filter is defined by optimizing a performance index which enhances real positive and real negative. The filter is used to minimize the probability of non-detected edge points and false detection.

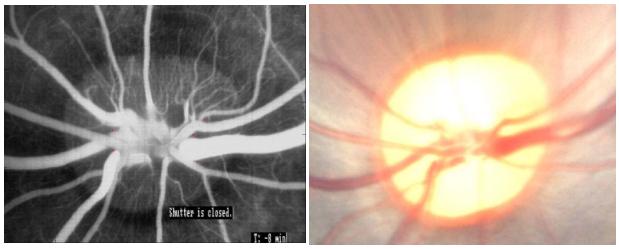

(a) (b)

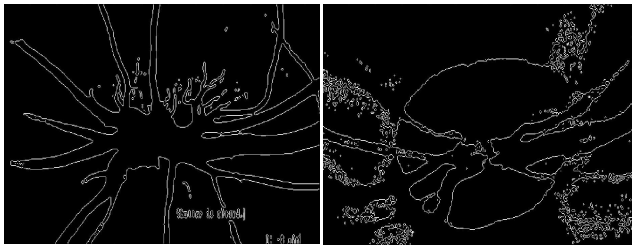

(c) (d)

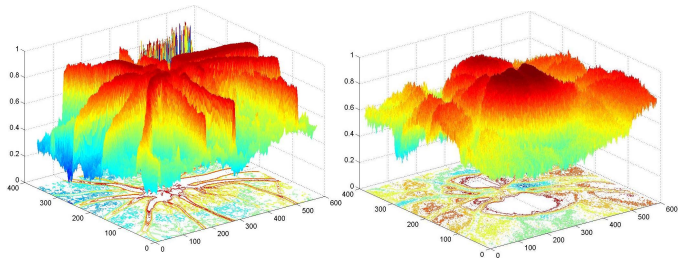

(e) (f)

Fig. 2. (a) – Reference image; (b) – Input image; (c) - Canny edges of the reference image; (d) – Canny edges of the input image; (e) – 3D shaded surface plot of the reference image; (f) – 3D shaded surface plot of the input image.

C. Control Point Detection

Good-guess of the initial control point selection ensures fused image generated at an efficient computational time. Bad control point selection will significantly increase the computation cost, or even cause the image fusion fail. Vessels or some particular abnormalities make images not necessarily matching the retina structures. Even when structure and function correspond, the abnormality still happens sometimes if inconsistence exists between structural and functional changes. Further more, angiogram images usually have higher resolution and are rich in information, whereas fundus images have lower resolution and are indeed abstract with some details or even missing some small vessels. Practically, those situations are unavoidable and will create difficulties in extracting the control points because the delineation of the vein boundaries may not be precise. In this study, control points are detected using the adaptive exploratory algorithm (Fig. 3 and Fig. 4) [12].

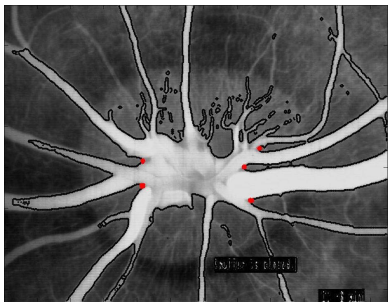

Fig. 3. Angiogram grayscale reference image's control point selection

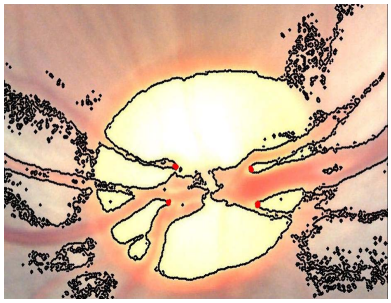

Fig. 4. Fundus true color input image's control point selection

IV. Heuristic Optimization Algorithm

A. Mutual-Pixel-Count (MPC) Objective Function

An optimization procedure is required to adjust the initial good-guess control points in order to achieve the optimal result (Fig. 5). The process can be formulated as a heuristic problem of optimizing an objective function that maximizes the Mutual-Pixel-Count between the reference and input images [6]. The algorithm finds the optimal solution by refining the transformation parameters in an ordered way. By maximizing the objective function, one image's vessels are supposed to be well overlaid onto those of the other image (Fig. 8) [10].

Mutual-Pixel-Count measures the optic nerve head vasculature overlapping for corresponding pixels in both images. It is assumed that the retinal vessels are represented by 0 (black pixel) and background is represented by 1 (white pixels) in the binary 2D map. When the vasculature pixel's transformed (u, v) coordinates on the input image correspond to the vasculature pixel's coordinates on the reference image, the MPC is incremented by 1 (Fig. 7). MPC is assumed be maximized when the image pair is perfectly geometrically aligned by the transformation. After pre-processing, the binary images of the reference and input images are obtained, i.e. I_{ref} and I_{input}. Only black pixels from both images contribute to MPC. The ideal case is that all zero pixels of the input image are mapped onto zero pixels of the reference image. The problem can be mathematically formulated as the maximization of the following objective function:

$$f_{mpc}(x,y,u,v) = \sum_{I_{ref}(x,y)=1 \text{ and } I_{input}(u,v)=1}^{u,v \in ROI} I_{input}(T_x(u,v), T_y(u,v)) \quad (5)$$

where f_{mpc} denotes the value of the Mutual-Pixel-Count. T_x and T_y are the transformations for u and v coordinates of the input image. The ROI (Region-of-Interest) is the vasculature region where the MPC is calculated on.

Ideally, f_{MPC} appears to contain a global maximum surrounded by the numerous local maxima. During the iteration, the reference image's control points' coordinates are fixed. Only input image's control points' coordinates are subject to adjustment.

Suppose ∇M is the changed volume of f_{MPC}, then:

$$\nabla M = MPC - MPC_{init} \Rightarrow \nabla M \begin{cases} > 0: & \text{Keep moving the coordinate toward the same direction} \\ \leq 0 & \text{Stop U or V coordinates' movement in that same direction} \end{cases}$$

Coordinates' adjustment is iteratively implemented until one of the following convergence criteria is reached:

(1). Predefined maximum number of loops is reached;
(2). the updated f_{MPC} is smaller than ε, i.e.

$$|f_{MPC}^{n+1}(x, y, u, v) - f_{MPC}^{n}(x, y, u, v)| < \varepsilon \quad (6)$$

where ε is a very small non-negative threshold.

B. Transformation Model

The 2D affine transformation model is applied to register the input image pixels into those of the reference image. The affine model has the capability to measure the lost information such as skew, translation, rotation, shearing and scaling that maps finite points to finite points and parallel lines to parallel lines.

$$\begin{pmatrix} U \\ V \\ 1 \end{pmatrix} = \begin{pmatrix} a_1 & a_2 & b_1 \\ a_3 & a_4 & b_2 \\ 0 & 0 & 1 \end{pmatrix} \begin{pmatrix} x \\ y \\ 1 \end{pmatrix} \quad (9)$$

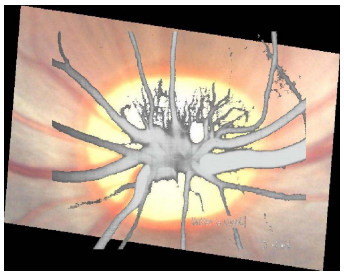

Fig. 5. Fused image prior to the optimization procedure

V. Evaluation Analysis – Compared with the Genetic Algorithm

Genetic Algorithms are well-known global optimization technique to solving the optimization problems [3][4]. Crossover and mutation are the two frequently used GA operations. There are totally 3 groups of the data populations, and each group stands for one control point from the input image. The population size remains same for each generation. Each individual is an unsigned char array. Array size (individual length) is a random number. The element in the array is the random number s_n that ranges from 0 to 3, standing for 4 possible moving directions (East, West, North and South). The initial 3 individuals are the coordinates of the initial guess of the control points ((x_1, y_1), (x_2, y_2), (x_3, y_3)). Each individual's fitness is estimated by the f_{MPC}. Half of the total individuals (parents + children) with higher f_{MPC} are selected. The offspring generation is iteratively produced till the termination condition is reached.

TABLE I

Comparison of GA and the Heuristic Algorithm's Average Performance

Optimization Algorithm	Average f_{MPC}	Running Time
GA	31830	7.4 minutes
Heuristic Algorithm	32277	1 minute

TABLE II

GA'S PERFORMANCE OF 20 RUNS

Run #	GA's f_{MPC}	Running Time
Run 1	31082	7.5 m
Run 2	31227	7.2 m
Run 3	31397	7.7 m
Run 4	31425	7.4 m
Run 5	31487	7.2 m
Run 6	31499	7.3 m
Run 7	31569	7.6 m
Run 8	31589	7.4 m
Run 9	32007	7.4 m
Run 10	32185	7.3 m
Run 11	32189	7.3 m
Run 12	32220	7.3 m
Run 13	32247	7.3 m
Run 14	31567	7.3 m
Run 15	31128	7.2 m
Run 16	32185	7.3 m
Run 17	31395	7.3 m
Run 18	32189	7.3 m
Run 19	31403	7.3 m
Run 20	29842	6.9 m

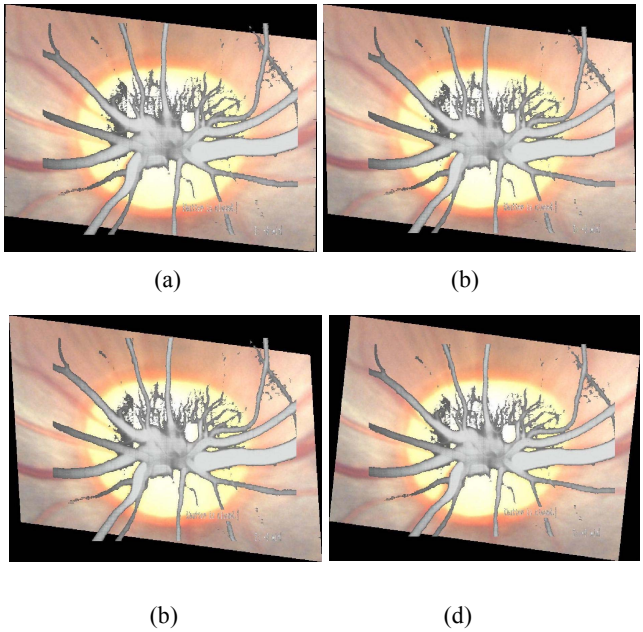

(a) (b)

(b) (d)

Fig. 6. Fused image generated by GA: (a) objective function f_{MPC} = 5981; (b) objective function f_{MPC} = 6095; (c) objective function f_{MPC} = 6300; (d) objective function f_{MPC} = 6471.

The experimental results showed that the proposed heuristic algorithm achieved better optimization (higher objective function f_{MPC}) than GA with less running time consumption (Table I) (Table II) (Fig. 6). Probably the most critical drawback of genetic algorithms is its strong dependence on a set of parameters (e.g., size of the population, number of generations, probabilities for applying the random operators, rate of generational reproduction, etc.) that have to be experimentally tuned for the optimization problem.

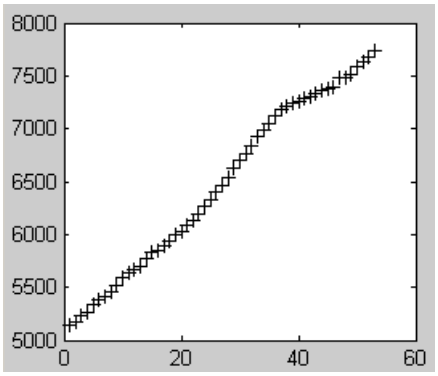

Fig. 7. f_{MPC} increasing during the iteration (Y-axis is f_{MPC}; X-axis is the loop count.

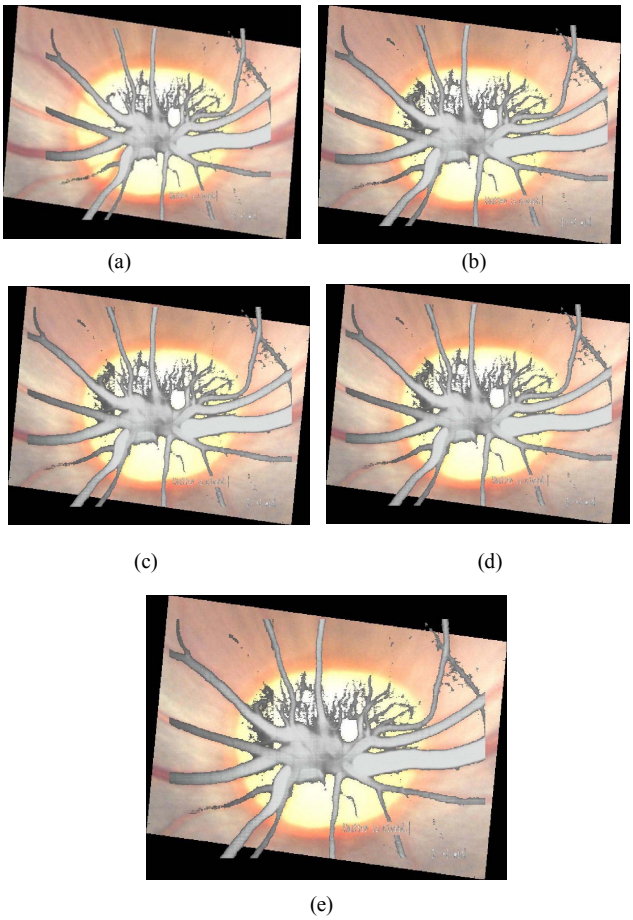

(a) (b)

(c) (d)

(e)

Fig. 8. Fused image improvement during the iteration. From (a)-(e) f_{MPC} = 5144, 7396, 7484, 7681, 7732

VI. CONCLUSIONS

The novel automated retinal image registration and fusion approach presented in this paper is efficient to handle multi-sensor retinal image registration and fusion as long as the input image, compared with the reference image does not have large rotation or translation. The genetic algorithm is compared with the heuristic optimization algorithm and the program running results shows that the heuristic algorithm has the advantage in terms of efficiency and accuracy. The continuous study plan is to evaluate the new algorithm in a larger experimental data of the control subjects. At this moment, it is difficult to find large quantity of monkey retinal image materials. Hopefully, this problem would be solved when more people and institutions are involved in the creation of the image materials.

REFERENCES

[1] F. Maes; A. Collignon; D. Vandermeulen; G. Marchal; P. Suetens; "Multimodality image registration by maximization of mutual information"; *IEEE Transactions on Medical Imaging*, V 16, N2, P 187-198, 1997.

[2] Z. Ye, H. Cao, S. Iyengar, H. Mohamadian; Chapter 6 - "Practical Approaches on Medical and Biometric System Identification for Pattern Recognition, Data Fusion and Information Measuring"; *Systems Engineering Approach to Medical Automation*; 2008.

[3] GK. Matsopoulos, NA. Mouravliansky, KK. Delibasis; "Automatic retinal image registration scheme using global optimization techniques"; *IEEE Transactions on Information Technology in Biomedicine*; V3, P47 - 60; Mar 1999.

[4] D. Doldberg; "Genetic Algorithms in Optimization"; *Search and Machine Learning*; *Reading*; MA; Addison-Wesley, 1989.

[5] J. Beach, J. Ning, B. Khoobehi; "Oxygen Saturation in Optic Neve Head Structures by Hyperspectral Image Analysis"; *Current Eye Research*; V32, P161-170, 2007.

[6] H. Cao, N. Brener, H. Thompson, S. S. Iyengar, Z. Ye; "Automated Control Point Detection, Registration, and Fusion at Fuzzy Retinal Vasculature Images", *IEEE 17th International Conference on Fuzzy Systems*; Hong Kong, China; P2386-2391; Jun.1-6, 2008. (IEEE-FUZZ 2008)

[7] N. Otsu; "A Threshold Selection Method from Gray-Level Histograms"; *IEEE Transactions on Systems, Man, and Cybernetics*; V9, P 62-66; 1979.

[8] P.K. Sahoo, A.A. Farag, Y. P. Yeap; "Threshold Selection Based on Histogram Modeling"; *IEEE Transactions on Systems, Man and Cybernetics*; V1, P 351 – 356, Oct 1992.

[9] J.F. Canny; "A computational approach to edge detection"; *IEEE Transactions on Pattern Analysis and Machine Intelligence*; V8, P 679-698; Nov. 1986.

[10] H. Cao, N. Brener, H. Thompson, S. S. Iyengar, Z. Ye; "Automated Registration and Fusion of the Multi-Modality Retinal Images"; *IEEE 40th Southeastern Symposium on System Theory*; New Orleans, LA, USA; P 371-375; March 16-18, 2008.

[11] B. Khoobehi, J. Beach, H. Kawano; "Hyperspectral imaging for measurement of oxygen saturation in the optic nerve head"; *Invest Ophthalmol Vis Sci*. V45, P1464–1472; 2004.

[12] H. Cao, N. Brener, H. Thompson, S. S. Iyengar, Z. Ye; "A Novel Automated Retinal Image Fusion Using Adaptive Exploratory Algorithm and Mutual-Pixel-Count Maximization"; *IEEE 40th Southeastern Symposium on System Theory;* New Orleans, LA, USA; P 122-126; March 16-18, 2008.